

ChemComm

Accepted Manuscript



This is an *Accepted Manuscript*, which has been through the Royal Society of Chemistry peer review process and has been accepted for publication.

Accepted Manuscripts are published online shortly after acceptance, before technical editing, formatting and proof reading. Using this free service, authors can make their results available to the community, in citable form, before we publish the edited article. We will replace this *Accepted Manuscript* with the edited and formatted *Advance Article* as soon as it is available.

You can find more information about *Accepted Manuscripts* in the [Information for Authors](#).

Please note that technical editing may introduce minor changes to the text and/or graphics, which may alter content. The journal's standard [Terms & Conditions](#) and the [Ethical guidelines](#) still apply. In no event shall the Royal Society of Chemistry be held responsible for any errors or omissions in this *Accepted Manuscript* or any consequences arising from the use of any information it contains.

ARTICLE

Bimolecular porous supramolecular networks deposited from solution on layered materials: graphite, boron nitride and molybdenum disulphide

Cite this: DOI: 10.1039/x0xx00000x

Received 00th January 2012,

Accepted 00th January 2012

DOI: 10.1039/x0xx00000x

www.rsc.org/

Vladimir V. Korolkov^a, Simon A. Svatek^a, Stephanie Allen^b, Clive J. Roberts^b, Saul J. B. Tendler^b, Takashi Taniguchi^c, Kenji Watanabe^c, Neil R. Champness^d and Peter H. Beton^{*a}

A two-dimensional porous network formed from perylene tetracarboxylic diimide (PTCDI) and melamine may be deposited from solution on the surfaces of highly oriented pyrolytic graphite (HOPG), hexagonal boron nitride (hBN) and molybdenum disulphide (MoS₂). Images acquired using high resolution atomic force microscopy (AFM) operating under ambient conditions has revealed that the network forms extended ordered monolayers (>1μm²) on HOPG and hBN whereas on MoS₂ much smaller islands are observed.

Coinage-metal surfaces and highly oriented pyrolytic graphite (HOPG) have been used in many of the studies of two-dimensional supramolecular organisation which have been reported over the past decade^{1–3}. These conducting substrates are compatible with scanning tunnelling microscopy (STM), and have structural properties which are understood in great detail, allowing experimental studies to focus on stabilisation of networks through hydrogen bonding^{4–8} and metal co-ordination^{9,10}. An extension of these studies to other substrates, particularly non-conducting surfaces, is highly desirable and would support investigations of a much wider range of properties going beyond the determination of structural and molecular organisation. The investigation of supramolecular networks on non-metallic substrates requires the use of atomic force microscopy (AFM) rather than STM. The potential of AFM for the acquisition of high resolution images of molecular structure has been convincingly demonstrated under ultra-high vacuum (UHV) conditions^{11–14}, including hydrogen-bonded systems^{15,16}, but to date AFM images of two-dimensional supramolecular organisation with molecular resolution have only been acquired under ambient conditions for trimesic acid¹⁷ and, using a torsional tapping mode, the bimolecular network formed by PTCDI (perylene tetracarboxylic di-imide) and melamine¹⁸; in these studies HOPG and gold, respectively, were used as substrates.

In this paper we show that, under ambient conditions, AFM images of supramolecular networks may be acquired with a resolution which is similar to that achieved using STM under the same conditions. A nanoporous honeycomb network formed from PTCDI and melamine network, previously studied on the Ag/Si(111)-surface under UHV conditions¹⁹, and on Au(111) first under UHV²⁰ and then from solution^{18,21} was chosen for this study. Recently the same network was formed on graphene multilayers grown on SiC under UHV conditions²². Here we compare the deposition of PTCDI and melamine from solution on three layered materials, HOPG, molybdenum disulphide (MoS₂) and exfoliated flakes of boron nitride (BN).

The molecular structures of PTCDI and melamine, together with the hydrogen-bonded PTCDI-melamine junction and the hexagonal

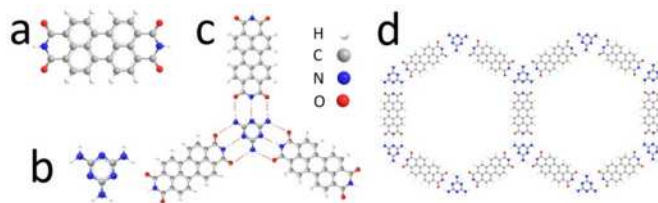


Fig. 1 Chemical structure of (a) PTCDI, (b) melamine; (c) schematic of PTCDI-melamine hydrogen bonded vertex, (d) unit cells of the derived supramolecular network.

unit cell of the resulting supramolecular structure are shown in Fig. 1. Each melamine interacts with three PTCDI molecules via a total of nine hydrogen bonds. We deposit the networks by immersion of the substrate into solutions of the molecular components which, as previous studies have shown for deposition on Au(111)^{18,21}, leads to much larger domains than those obtained by UHV deposition.

Images of the networks are acquired using AFM, which for the layers deposited on graphite may be complemented by STM. In this work we use, predominantly, PeakForce tapping mode AFM, which was recently introduced by Bruker. In this mode the tip oscillates at a frequency far below resonance and a force-distance curve is acquired at each pixel. The maximum force detected during the approach cycle is used as a set point which, in conjunction with a feedback loop, regulates the probe height. The values for the set point are typically in the (repulsive) range of 1-10 pN, allowing for a very low force while imaging delicate systems. As the force curve is recorded at every single pixel it is also possible to determine the spatial variation of mechanical properties, such as adhesion, of the array. AFM images were acquired in ambient conditions using standard silicon tips (Multi75Al, Multi75Al-G supplied by Budget Sensors; typical spring constant, 2.8 N/m). We have also used a Cypher AFM (Asylum Research) to acquire images (in tapping mode) of some samples. STM imaging was performed utilizing tips cut from Pt/Ir (20% Ir) wire. WsXM V5.0 software was used to process and analyse all AFM images²³.

The PTCDI-melamine network was prepared via adsorption in a dimethylformamide (DMF) solution at 373K^{18,21}. The melamine and PTCDI concentrations were 0.66 mM and ~0.5 μM respectively. Each sample was rinsed with 5 ml of fresh DMF and blown dry in N₂-stream. The same protocol was used for all substrates.

Figure 2 shows AFM images following molecular deposition on HOPG (purchased from NT-MDT (20 minute immersion time)). The AFM images show clearly that a regular hexagonal framework is formed on the HOPG surface with the structure and dimensions expected for the PTCDI-melamine network shown in Fig. 1. Fig. 2a shows a hexagonal array of nanopores in a single domain which extends over 250 nm (in larger area images we observe islands with dimensions up to 0.5 μm; see Electronic Supplementary Information (ESI)). The size of these domains, and the fraction of the surface covered (>90%) by the network is much greater than

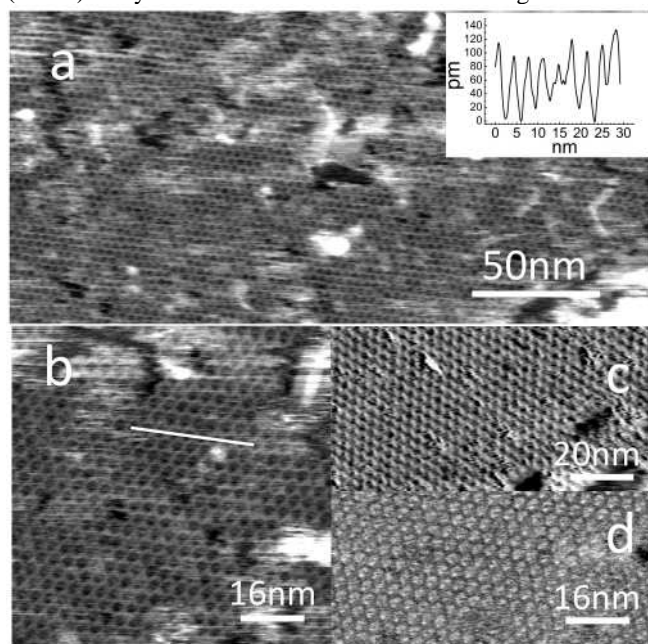


Fig. 2 AFM and STM scans of a PTCDI-melamine network on HOPG in air. Images **a** and **b** are topographic AFM scans. Image **c** is a constant current STM image acquired at $I = 5$ pA and sample voltage 0.5V. Image **d** shows adhesion distribution of the upper half of the area in **b**. Inset on image **a** shows cross-section taken along the line shown in image **b**.

that achieved in previous UHV studies^{19,20,22}, but is comparable to those previously reported for solution deposition on Au(111)^{18,21}. The measured lattice constant is 3.5 ± 0.1 nm, very close to the values of 3.46 nm and 3.5 nm reported for adsorption on Ag/Si(111)¹⁹ and Au(111)^{20,21} surfaces. A height profile extracted from a higher magnification image (Fig. 2b) is shown in the inset; the topographic height of the molecules is ~0.1 nm. Fig. 2c shows, for comparison, an STM image of a surface prepared using the same (highly reproducible) protocol. Interestingly, there is very little difference between the resolution and image quality using these two modalities (see ESI for additional images).

Fig. 2d shows an adhesion map which is extracted from the force-distance curves measured during the acquisition of Fig. 2b; the adhesion is defined as the maximum attractive force during the retraction of the cantilever. This image shows stronger adhesion at the centres of the hexagonal cavities formed in the array, where the

HOPG surface is exposed, with the network structure appearing as a dark honeycomb mesh (darker features correspond to lower adhesion). Similar behaviour was observed for trimesic acid monolayers adsorbed on HOPG¹⁷. At this stage a quantitative interpretation, which requires detailed knowledge of the probe radius, is not possible. However, we include these observations to highlight the potential for AFM to provide additional modalities in future studies of host-guest interactions in supramolecular networks.

We have also successfully deposited the PTCDI-melamine network on hBN. These surfaces are prepared by exfoliating hBN flakes from small mm-sized crystals grown at the National Institute for Materials Science, and transferring them to a silicon wafer on which a 300 nm thick oxide layer has been grown. The flakes are then heated in an Ar/H₂ (95:5) atmosphere at 400 °C for 4-6 hours to remove organic residues. This process is very similar to that used by other researchers to prepare hBN substrates for use in graphene research^{24,25}. hBN is a layered compound with a structure similar to graphite, except that the two atom carbon basis set is replaced by two heteroatoms, boron and nitrogen. As a large band-gap semiconductor hBN is not suitable for study with STM and all images were acquired using AFM.

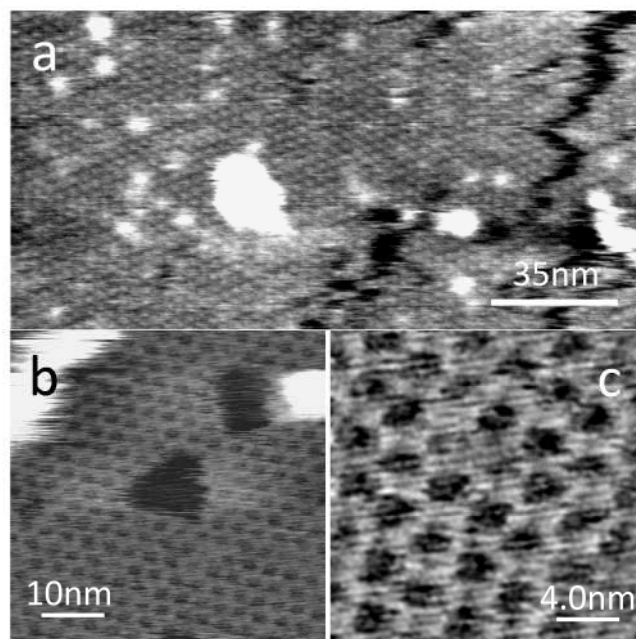


Fig. 3 AFM scans of the PTCDI-melamine network on the hBN surface in air. Image **a** was acquired in tapping mode on a Cypher AFM (Asylum Research). Images **b** and **c** were taken in PeakForce Tapping Mode.

The PTCDI-melamine network could be readily formed on this substrate by immersion in the solution described above for 1 minute; this was found to be sufficient to grow an extended monolayer of the network with typical islands with widths ~0.3 μm (see ESI). Fig. 3a shows a large area image in which the honeycomb lattice is clearly resolved and we determine the lattice constant as 3.5 ± 0.1 nm, the same value, within experimental error as observed for the network on HOPG. Higher magnification images acquired in PeakForce tapping mode which show the honeycomb network are presented in Figs 3b-c. In both Figs 3a and b there are darker features with faceted edges which appear within the molecular network. These are defects in the

molecular layer and tend to grow during the acquisition of AFM images, so that after prolonged imaging the network becomes discontinuous.

MoS₂ is a layered semiconductor currently attracting interest due to its potential for integration with graphene²⁶. We have also demonstrated that the PTCDI-melamine network may be formed on this surface as shown in Figure 4. A similar protocol is used as for the formation on HOPG and hBN, but on the MoS₂ surface much smaller islands are formed. After a deposition time of 1 minute we see only islands of typical lateral dimensions of < 100 nm. Increase of the immersion time to 10 minutes leads to the formation of an extended supramolecular layer with a hexagonal symmetry and a lattice

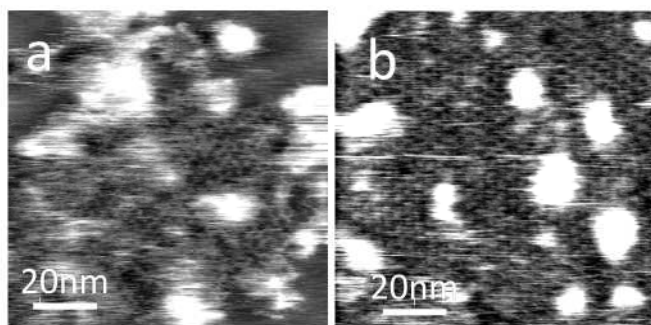


Fig. 4 AFM images of PTCDI-melamine network on MoS₂ surface after a – 1 minute and b – 10 minute adsorption times.

constant of 3.5 ± 0.1 nm consistent with the formation of the hydrogen-bonded structure in Fig. 1. We have also tried to image this surface using STM but have not succeeded in acquiring images showing the molecular network.

The most significant difference which we identify for adsorption on MoS₂ lies in the dimensions of the network. This may be due to differences in chemistry; in particular the presence of a layer of sulphur atoms at the surface may lead to stronger interactions with both environmental gaseous species, and also with the adsorbed molecules themselves. Nevertheless, our results confirm that the hydrogen-bonding which leads to the stabilisation of the honeycomb network is effective on the MoS₂ surface.

The network co-exists with three dimensional features for which we cannot obtain molecular resolution; these may be due to adsorption of molecules in a non-planar configuration, or, possibly, the formation of multilayers, and are present in slightly greater concentration on the MoS₂ surface. Possibly due to the smaller islands and greater disorder observed on this surface, it is more difficult to acquire images, and we have not been able to acquire adhesion maps with nm-scale MoS₂ substrates (adhesion maps for hBN are included in the ESI; these show a similar contrast to Fig. 2d). For all substrates the network structure remains sufficiently stable when kept in a sealed vial filled with nitrogen for further images to be obtained for over a week.

Conclusions

In our study we have successfully demonstrated that hydrogen-bonded supramolecular networks can be readily deposited on the surfaces of HOPG, hBN and MoS₂. Importantly the structures may be resolved using AFM using conventional micromachined cantilevers. The formation of the honeycomb PTCDI-melamine network and its stability under ambient conditions is particularly important since this offers the

prospect of integrating molecular recognition and host-guest interactions with a family of layered materials, including semimetals, semiconductors and insulators, which are currently receiving great attention as candidates for a new generation of optoelectronic devices^{26,27}.

Acknowledgements

Financial support was provided by the UK Engineering and Physical Sciences Research Council (EPSRC; grants EP/K01773X/1 and EP/K005138/1).

^a School of Physics & Astronomy, The University of Nottingham, Nottingham NG7 2RD, UK. E-mail: peter.beton@nottingham.ac.uk

^b School of Pharmacy, The University of Nottingham, Nottingham, NG7 2RD, UK

^c The National Institute for Materials Science, Advanced Materials Laboratory, 1-1 Namiki, Tsukuba, Ibaraki 305-0044, Japan

^d School of Chemistry, The University of Nottingham, Nottingham NG7 2RD, UK

Electronic Supplementary Information (ESI) available: additional images of network. See DOI: 10.1039/c000000x/

Notes and references

1. L. Bartels, *Nat. Chem.*, 2010, **2**, 87–95.
2. T. Kudernac, S. Lei, J. A. A. W. Elemans, and S. De Feyter, *Chem. Soc. Rev.*, 2009, **38**, 402–21.
3. A. G. Slater (née Phillips), P. H. Beton, and N. R. Champness, *Chem. Sci.*, 2011, **2**, 1440.
4. J. V Barth, J. Weckesser, C. Cai, P. Günter, L. Bürgi, O. Jeandupeux, and K. Kern, *Angew. Chemie Int. Ed.*, 2000, 1230–1234.
5. S. B. Lei, C. Wang, S. X. Yin, H. N. Wang, F. Xi, H. W. Liu, B. Xu, L. J. Wan, and C. L. Bai, *J. Phys. Chem. B*, 2001, **105**, 10838–10841.
6. S. Griessl, M. Lackinger, M. Edelwirth, M. Hietschold, and W. M. Heckl, *Single Mol.*, 2002, **3**, 25–31.
7. K. G. Nath, O. Ivasenko, J. A. Miwa, H. Dang, J. D. Wuest, A. Nanci, D. F. Perepichka, and F. Rosei, *J. Am. Chem. Soc.*, 2006, **128**, 4212–3.
8. D. L. Keeling, N. S. Oxtoby, C. Wilson, M. J. Humphry, N. R. Champness, and P. H. Beton, *Nano Lett.*, 2003, **3**, 9–12.
9. S. Stepanow, M. Lingenfelder, A. Dmitriev, H. Spillmann, E. Delvigne, N. Lin, X. Deng, C. Cai, J. V Barth, and K. Kern, *Nat. Mater.*, 2004, **3**, 229–33.
10. A. Dmitriev, H. Spillmann, N. Lin, J. V Barth, and K. Kern, *Angew. Chem. Int. Ed. Engl.*, 2003, **42**, 2670–3.
11. L. Gross, F. Mohn, N. Moll, P. Liljeroth, and G. Meyer, *Science*, 2009, **325**, 1110–4.
12. P. Rahe, R. Lindner, M. Kittelmann, M. Nimmrich, and A. Kühnle, *Phys. Chem. Chem. Phys.*, 2012, **14**, 6544–8.
13. S. Burke, J. Mativetsky, S. Fostner, and P. Grütter, *Phys. Rev. B*, 2007, **76**, 035419.
14. S. Maier, L.-A. Fendt, L. Zimmerli, T. Glatzel, O. Pfeiffer, F. Diederich, and E. Meyer, *Small*, 2008, **4**, 1115–8.
15. J. Zhang, P. Chen, B. Yuan, W. Ji, Z. Cheng, and X. Qiu, *Science*, 2013, **342**, 611–4.
16. A. M. Sweetman, S. P. Jarvis, H. Sang, I. Lekkas, P. Rahe, Y. Wang, J. Wang, N. Champness, L. Kantorovich, and P. Moriarty, *Nat. Commun.*, 2014, in press.
17. V. V. Korolkov, S. Allen, C. J. Roberts, and S. J. B. Tendler, *J. Phys. Chem. C*, 2012, **116**, 11519–11525.
18. V. V. Korolkov, N. Mullin, S. Allen, C. J. Roberts, J. K. Hobbs, and S. J. B. Tendler, *Phys. Chem. Chem. Phys.*, 2012, **14**, 15909.
19. J. A. Theobald, N. S. Oxtoby, M. A. Phillips, N. R. Champness, and P. H. Beton, *Nature*, 2003, **424**, 1029–31.
20. L. M. A. Perdigão, E. W. Perkins, J. Ma, P. A. Staniec, B. L. Rogers, N. R. Champness, and P. H. Beton, *J. Phys. Chem. B*, 2006, **110**, 12539–42.
21. R. Madueno, M. T. Räisänen, C. Silien, and M. Buck, *Nature*, 2008, **454**, 618–21.

22. H. J. Karmel, T. Chien, V. Demers-Carpentier, J. J. Garramone, and M. C. Hersam, *J. Phys. Chem. Lett.*, 2014, **5**, 270–274.
23. I. Horcas, R. Fernández, J. M. Gómez-Rodríguez, J. Colchero, J. Gómez-Herrero, and A. M. Baro, *Rev. Sci. Instrum.*, 2007, **78**, 013705.
24. C. R. Dean, A. F. Young, I. Meric, C. Lee, L. Wang, S. Sorgenfrei, K. Watanabe, T. Taniguchi, P. Kim, K. L. Shepard, and J. Hone, *Nat. Nanotechnol.*, 2010, **5**, 722–6.
25. M. Yankowitz, J. Xue, D. Cormode, J. D. Sanchez-Yamagishi, K. Watanabe, T. Taniguchi, P. Jarillo-Herrero, P. Jacquod, and B. J. LeRoy, *Nat. Phys.*, 2012, **8**, 382–386.
26. A. K. Geim and I. V Grigorieva, *Nature*, 2013, **499**, 419–25.
27. T. Georgiou, R. Jalil, B. D. Belle, L. Britnell, R. V Gorbachev, S. V Morozov, Y.-J. Kim, A. Gholinia, S. J. Haigh, O. Makarovsky, L. Eaves, L. a Ponomarenko, A. K. Geim, K. S. Novoselov, and A. Mishchenko, *Nat. Nanotechnol.*, 2013, **8**, 100–3.